Scientific Research Publishing

Open Journal of Modelling and Simulation, 2025, 13(4), 185-195
https://www.scirp.org/journal/ojmsi
ISSN Online: 2327-4026
ISSN Print: 2327-4018

Pulsatile Flow Hemodynamics in a Stenosed Artery for Newtonian and Non-Newtonian Rheological Models

Md. Jashim Uddin

Department of Applied Mathematics, Noakhali Science and Technology University, Noakhali, Bangladesh
Email: mdjaud11@gmail.com

How to cite this paper: Uddin, Md.J. (2025) Pulsatile Flow Hemodynamics in a Stenosed Artery for Newtonian and Non-Newtonian Rheological Models. *Open Journal of Modelling and Simulation*, **13**, 185-195.
https://doi.org/10.4236/ojmsi.2025.134010

Received: July 15, 2025
Accepted: August 26, 2025
Published: August 29, 2025

Abstract

Atheromatous disease can cause a heart attack or stroke in humans. This present research aims to investigate the comparison between Newtonian and rheological models in terms of hemodynamic risk factors. A three-dimensional computational model has been considered here for 45%, 60%, and 75% stenoses. The COMSOL Multiphysics software has been used in fluid flow simulation to solve the governing equations. The comparison between Newtonian and non-Newtonian has been performed to predict the model's suitability. Hemodynamic parameters such as time-averaged wall shear stress (TAWSS), oscillatory shearing index, and blood residence time show a lower disturbed flow regime for non-Newtonian fluid compared to Newtonian fluid. The TAWSS for 75% stenosis is increased by 54.84% and 37.18% to those of 45% and 60% stenoses. A suitable non-Newtonian model can be used in bioengineering fields.

Keywords

Pulsatile Flow, Stenosis, Hemodynamics, Recirculation, Non-Newtonian Rheological Model

1. Introduction

One of the main causes of illness and death worldwide is cardiovascular disorder. Arterial blockage is a disorder in which plaque builds up in the arteries and causes them to narrow, leading to decreased blood flow [1]-[5]. Due to the blood flow's straight connection to cardiovascular health, research on it via narrowed arteries has attracted a lot of attention. The aforementioned arteries have extremely complicated blood flow that is affected by a number of variables, including the stenosis's shape, the blood's characteristics, and the existence of disorder [6]-[10]. Custom-

arily, blood is treated as a Newtonian fluid, presuming a uniform viscosity that does not change with shear rate. In actuality, though, blood behaves with non-Newtonian characteristics, changing viscosity in response to shear rate, especially in narrow lumens or in sick circumstances [11]-[15].

The evaluation of changes in hemodynamic risk factors across various viscosity models has made extensive use of computational fluid dynamics (CFD) simulations [16] [17]. Important hemodynamic risk factors that are essential for comprehending how blockage affects blood circulation include wall shear stress (WSS), time-averaged wall shear stress (TAWSS), oscillatory shear index (OSI), and relative residence time (RRT) [18]-[20]. This study seeks to examine the influences of the nature of Newtonian and non-Newtonian fluids on the hemodynamic flow properties within constricted vessels. Because of Newtonian fluids' straightforwardness, they have been widely employed in the past years [21]-[24]. In order to better comprehend the types of flow, non-Newtonian model—specially, the Carreau model—has been suggested as a more factual description of the rheological characteristics of blood [25]-[27].

The stenosed geometry has been found to have an important impact on blood flow-related research. A significant volume of research has focused on comprehending blood circulation in arteries, in both normal and narrowed states. Past research shows that the Newtonian model is widely utilized because of its ease. In this present computational investigation, the study seeks to explore the impacts of the variational approach of Newtonian and non-Newtonian fluids on the hemodynamic flow behaviors in narrowed arteries. This study also intends to show the great impact of the severity of stenosis on flow fields.

2. Methodology Techniques

2.1. Simulated Geometry

A stenosed model of three-dimensional geometry (**Figure 1**) for 45%, 60%, and 75% stenoses has been considered here to investigate the pulsatile atherosclerotic hemodynamics in mimics blood flow. The directions of the horizontal and vertical axes are shown by the coordinates X and Y. The length of pre-stenosis is 3D and the post-stenosis is 10D. The parameter D indicates the artery diameter. The laminar and incompressible flow is assumed for the investigated trapezium model of stenosis.

2.2. Governing Equations and Boundary Conditions

The fluid flow simulations are governed by the continuity and Navier-Stokes equations, as given in the following way:

The general continuity equation's form for fluid flow is

$$\nabla \cdot \boldsymbol{v} = 0 \tag{1}$$

The Navier-Stokes equations' form is

$$\rho\left(\frac{\partial \boldsymbol{v}}{\partial t} + (\nabla \cdot \boldsymbol{v})\boldsymbol{v}\right) = \nabla \cdot \boldsymbol{\sigma} \tag{2}$$

where $\boldsymbol{v}$ is the velocity vector, t is the time, ρ indicates the density of the fluid,

and p is the fluid pressure. The Cauchy stress tensor σ can be given as follows:

$$-PI+\mu\left(\nabla \boldsymbol{v}+(\nabla \boldsymbol{v})^{\mathrm{T}}\right)$$

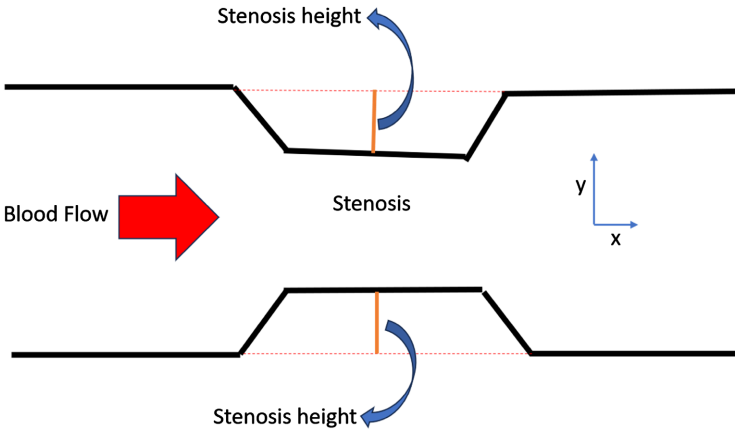

Figure 1. The current simulation domain.

where μ presents the dynamic viscosity of the fluid, and I is the identity matrix. The non-Newtonian Carreau model is as follows:

$$\mu=\mu_{\inf}+\left(\mu_0-\mu_{\inf}\right)\left[1+\left(\lambda\frac{\partial\gamma}{\partial t}\right)^2\right]^{\frac{n-1}{2}}$$

where infinite shear rate $\mu_{\inf}=0.00345$, zero shear rate $\mu_0=0.056$, time constant $\lambda=3.313$, and index $n=0.3568$. The pulse given in Figure 2 presents the

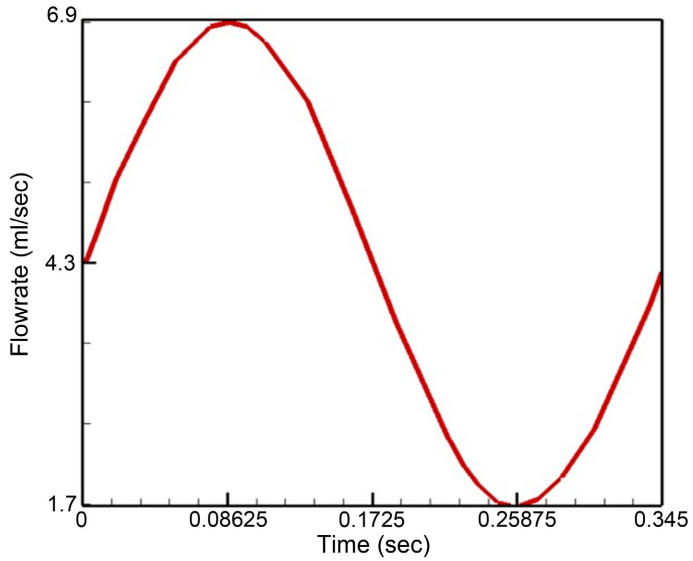

Figure 2. Time-dependent input flowrate pulse.

inlet flowrate pulse for the present computational fluid model [28]. A no-slip boundary condition is applied at the wall, while the outlet pressure remains static. The pulsatile flow exhibits a waveform of 4.3 ± 2.6 ml with a duration of 0.345 s, pro-

duced by a frequency of 2.9 Hz. The fluid has a density of 755 kg/m^3 and a viscosity of 0.00143 N·s/m^2. The inlet pulse is a sinusoidal wave with an average Reynolds number of 575 and a peak value of 930 [29].

2.3. Numerical Methods

Newtonian and non-Newtonian rheological models have been assumed for incompressible, laminar and time-dependent flow. The finite element approach in the COMSOL Multiphysics software has been activated for numerical computational techniques. Time-dependent solver takes the fully coupled, advanced and iterative approach for the execution of pulsatile blood flow simulation. Different mesh densities, namely 36,405, 80,542, 107,835, 206,940, and 307,560, have been selected to decide the appropriate mesh for the prediction of outcomes. The mesh elements of 206,940 are appropriate to acquire the results because the last two elements, 206,940 and 307,560, carry approximately the same TAWSS magnitudes. **Figure 3(a)** shows the grid, and **Figure 3(b)** presents the grid test in TAWSS. In unsteady flow, the second cycle has been taken to get the simulated results.

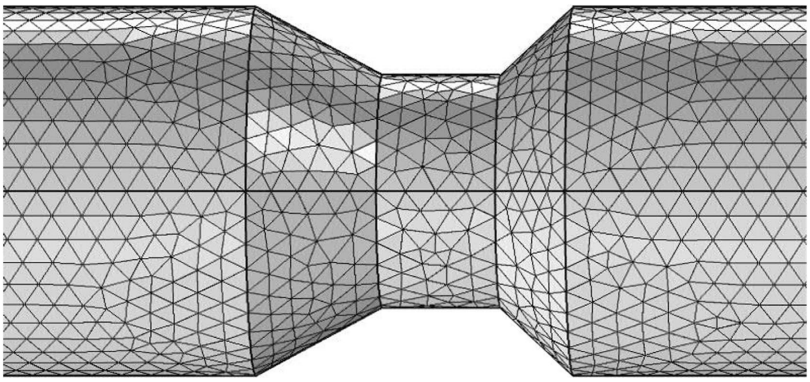

(a)

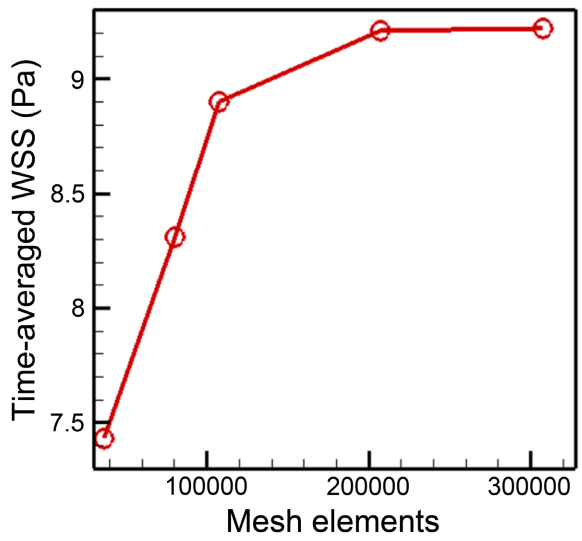

(b)

Figure 3. (a) Grid resolution and (b) grid independence test in TAWSS.

2.4. Method Validation

In the present research, axial velocity through the radial direction is employed to contrast the results with those of Lee *et al.* [30], aiming to verify and affirm the precision and reliability of the computational evaluation. The axial velocity is taken as a post-stenotic distance of 21.5 mm at $t = 0.1725$ sec. Moreover, as shown in **Figure 4**, the comparison of the currently predicted axial velocity results with those obtained by Lee *et al.* [30] demonstrates significant agreement.

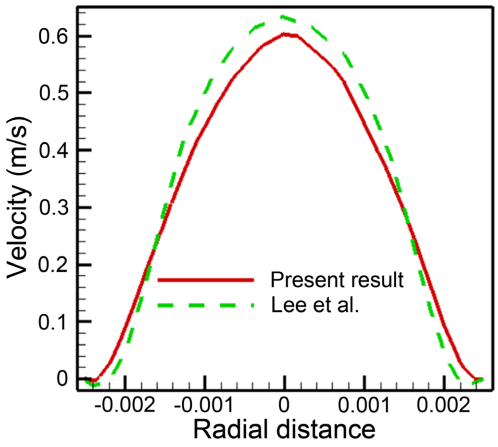

Figure 4. Axial velocity through radial direction is validated with Lee *et al.* [30].

3. Results and Discussion

3.1. Hemodynamic Biomarker Factors' Impact

WSS is the key hemodynamic factor that signifies the level of risk for patients. Elevated WSS is associated with the development of susceptible plaques, whereas diminished WSS may result in intimal thickening. **Figure 5** illustrates the distributions of WSS with noticeable variations of Newtonian and non-Newtonian fluids at various significant time points ($t = 0.08623$ s, $t = 0.1725$ s, $t = 0.25875$ s, $t = 0.345$ s). Since the flow directly affects the stenosis's inlet region, the WSS peaks there, WSS then abruptly increases, remains somewhat elevated throughout the constricted region, and then decreases from the terminating regions. While both fluids result in elevated WSS close to the narrowed portion, the rheological non-Newtonian model generates a greater WSS at every site except the closely post-stenotic part. The Newtonian fluid exhibits a higher recirculation in the area immediately downstream of the blockage than the rheological fluid. The arterial wall displays time-averaged markers such as TAWSS, OSI, and RRT, serving as indicators of endothelial deterioration (**Figures 6(a)-(c)**). The top values of OSI and RRT signify the reattachment locations, which align with zero for TAWSS, and Newtonian fluid gives a more disturbed flow area.

3.2. Stenosis Severity's Impact on Hemodynamics

Without a doubt, the intensity or size significantly influences the flow area of the narrowed channels of blockage. To examine the impact of stenosis intensity, three

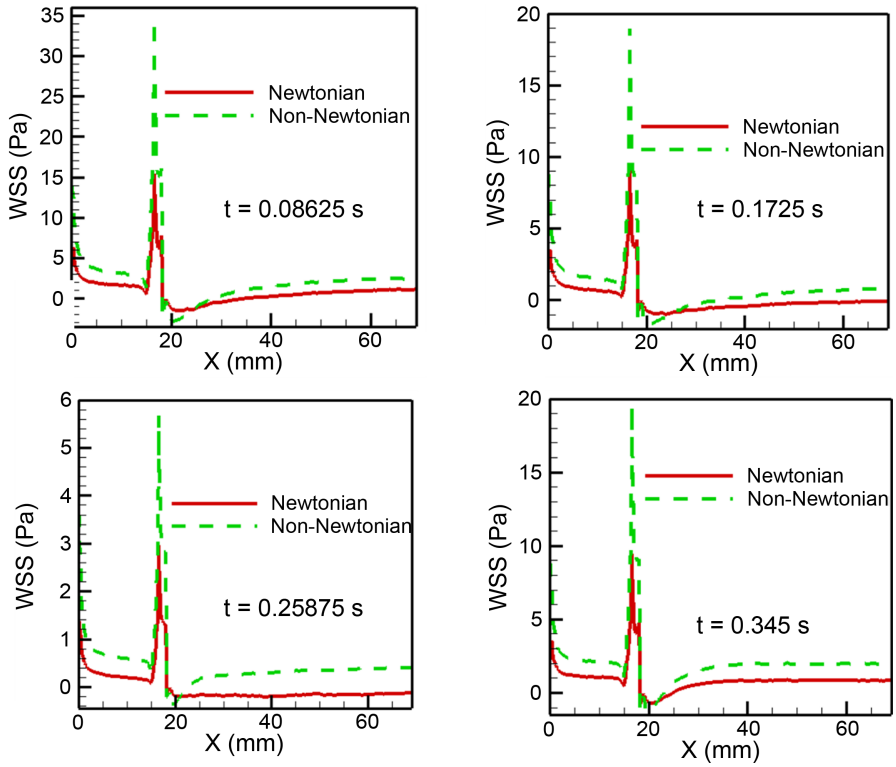

Figure 5. WSS distributions at (t = 0.08625 s, 0.1725 s, 0.25875 s, and 0.345 s) for Newtonian and non-Newtonian fluids.

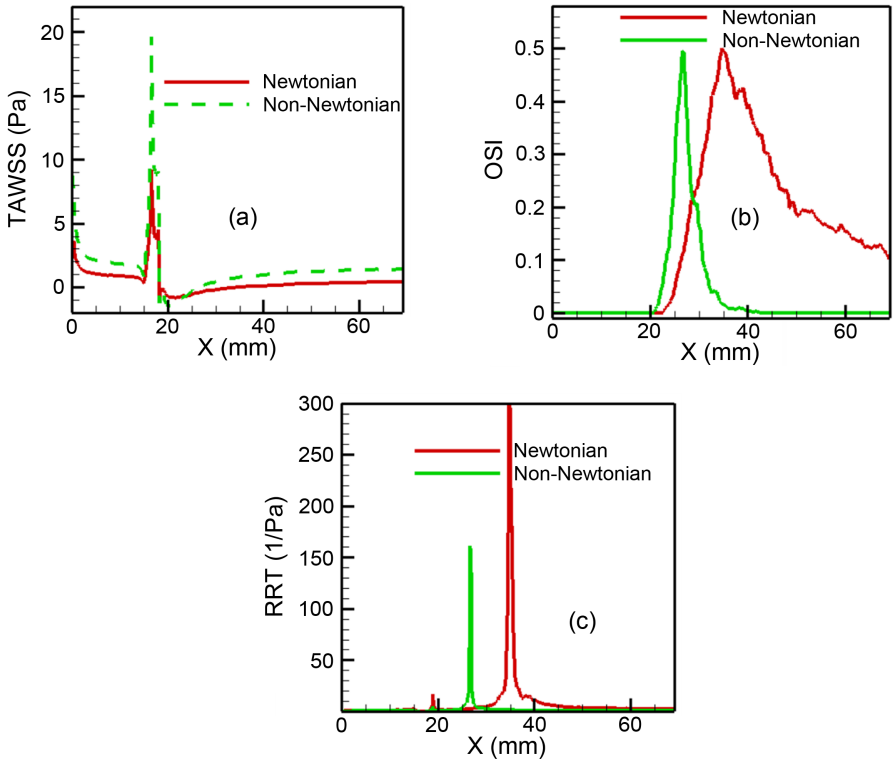

Figure 6. Distributions of (a) TAWSS, (b) OSI, and (c) RRT for Newtonian and non-Newtonian fluids.

distinct sizes, specifically 45%, 60%, and 75% (Figure 7(a)), have been analyzed in terms of WSS. As the severity of the blockage deepens, the flow field diminishes, resulting in an increase in velocity, which significantly affects the WSS, leading to a peak in the WSS due to the acceleration of flow. The TAWSS for 75% stenosis rises by 54.84% and 37.18% compared to 45% and 60% stenoses, respectively. Finally, it may be concluded that the more vascular injury generates the more WSS. Figure 7(b) presents the contours of WSS distributions for the various sizes of blockage severity. At the stenosis location, the flow area is reduced and experiences a maximum shearing stress. The higher blockage (75%) attains a maximum value of WSS compared to the lower blockages.

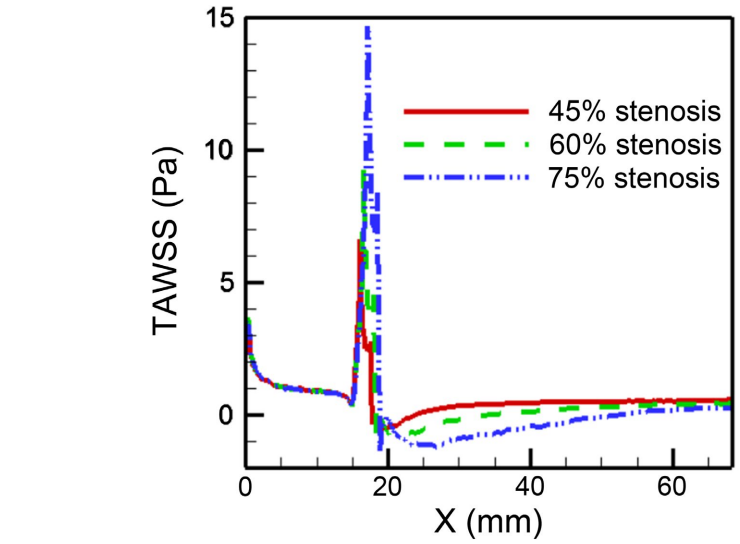

(a)

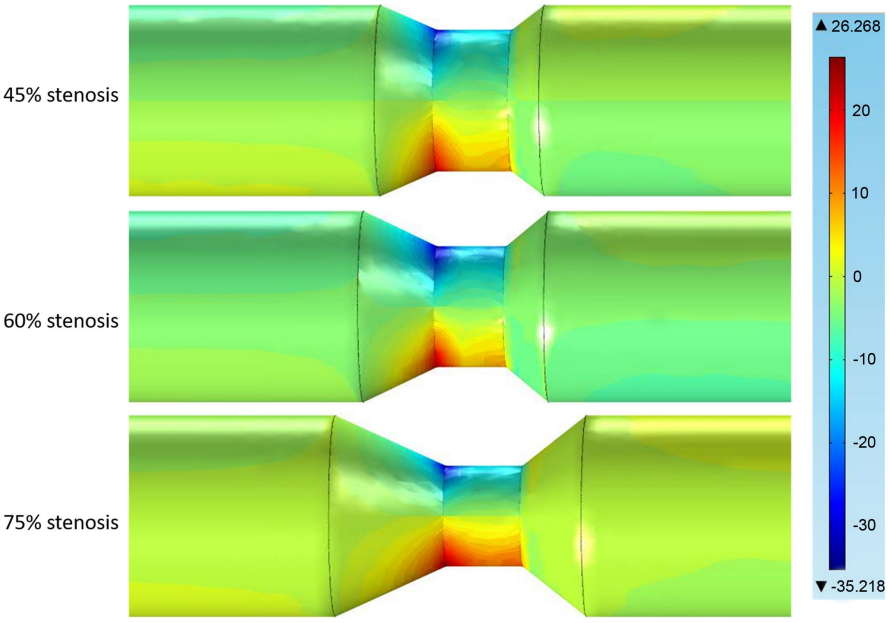

(b)

Figure 7. (a) Distribution of TAWSS and (b) WSS contours for 45 %, 60%, and 75%.

3.3. Pressure Contours Due to Newtonian and Non-Newtonian Fluids

Pressure distributions for Newtonian and rheological models may vary greatly because of their different viscosities and responses to shear stress. The comparison of pressure contours between the two aforementioned models reveals a significant difference in Figure 8, in which the non-Newtonian model generates greater pressure. The artery's initial higher pressure drops sharply at the blockage's midpoint, followed by a gradual rise until the artery's end, indicating a slight variation between the fluids. The lowest pressure is observed just downstream of the blockage, suggesting a condition favorable to the development of atherosclerosis.

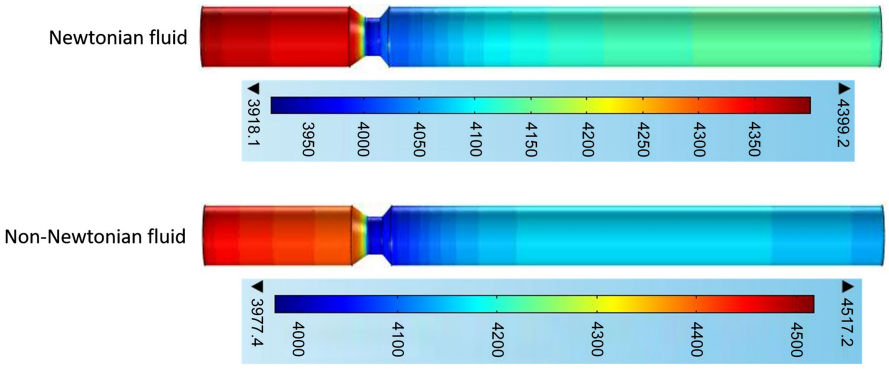

Figure 8. Pressure contour distributions for Newtonian and non-Newtonian fluids.

4. Conclusions

Atherosclerosis is associated with blood flow characteristics and the intensity of constriction in the arterial lumen and the walls of the arterial geometry, making it essential to examine blood circulation in a diseased arterial geometry. In order to demonstrate the laminar, pulsating, and incompressible blood flow in an injured artery, the current work used CFD modeling. The Newtonian and Carreau models of blood have both been taken into consideration in this study. The code of COMSOL Multiphysics is validated with literature findings. The applicability of the model has been predicted by comparing Newtonian and non-Newtonian models. When comparing non-Newtonian fluids to Newtonian fluids, hemodynamic metrics, including TAWSS, OSI, and RRT, reveal a reduced disturbed flow regime. Compared to 45% and 60% stenosis, the TAWSS for 75% stenosis is raised by 54.84% and 37.18%, respectively. An appropriate non-Newtonian model can be applied in the field of bioengineering.

In the future, the rigid wall geometry assumptions can be extended to a realistic patient-specific fluid-structure interaction model.

Conflicts of Interest

The author declares no conflicts of interest regarding the publication of this paper.

References

[1] Akbar, S. and Shah, S.R. (2024) Mathematical Modeling of Blood Flow Dynamics in

the Cardiovascular System: Assumptions, Considerations, and Simulation Results. *Journal of Current Medical Research and Opinion*, **7**, 2216-2225.

[2] Anamika Shah, S.R. and Singh, A. (2017) Mathematical and Computational Study of Blood Flow through Diseased Artery. *International Journal of Computer Science*, **5**, 1-6.

[3] Dutt, M.G., Shah, S.R. and Arya, S. (2024) Optimizing Cardiovascular Health: Ayurvedic Insights into Blood Flow through Normal and Stenosed Arteries. *International Journal of AYUSH*, **13**, 18-35.

[4] Udupa, M.C., Saha, S. and Natarajan, S. (2025) Study of Blood Flow Patterns in a Stenosed Artery through the Combined Effect of Body Acceleration and Generalized Womersley Solution. *Scientific Reports*, **15**, Article No. 1845. https://doi.org/10.1038/s41598-025-85566-2

[5] Shah, S.R., Siddiqui, S.U. and Singh, A. (2015) Mathematical Modelling and Analysis of Blood Flow through Diseased Blood Vessels. *International Journal of Engineering and Management Research*, **5**, 366-372.

[6] Singh, S. and Shah, R.R. (2010) A Numerical Model for the Effect of Stenosis Shape on Blood Flow through an Artery Using Power-Law Fluid. *Advance in Applied Science Research*, **1**, 66-73.

[7] Shah, S.R. and Kumar, R. (2017) A Mathematical Approach to Study the Blood Flow through Tapered Stenosed Artery with the Suspension of Nanoparticles. *DEStech Transactions on Engineering and Technology Research*, **1**, 1-6. https://doi.org/10.12783/dtetr/amsm2017/14809

[8] Shah, S.R. (2013) A Mathematical Model for the Analysis of Blood Flow through Diseased Blood Vessels under the Influence of Porous Parameter. *Journal of Biosciences and Technology*, **4**, 534-541.

[9] Singh, A. and Shah, S.R. (2024) Influence of Transverse Magnetic Field on Steady Blood Flow in a Stenosed Artery: Numerical and Analytical Insights. *International Journal of Mathematical Archive*, **15**, 1-10.

[10] Kumar, V. and Shah, S.R. (2022) A Mathematical Study for Heat Transfer Phenomenological Processes in Human Skin. *International Journal of Mechanical Engineering*, **7**, 683-692.

[11] Sapna, K. and Siddiqui, S.U. (2004) Study of Blood Flow through a Stenosed Capillary Using Casson's Fluid Model. *Ultra Science*: *International Journal of Physical Sciences*, **16**, 133-142.

[12] Sapna, S. (2009) Analysis of Non-Newtonian Fluid Flow in a Stenosed Artery. *International Journal of Physical Sciences*, **4**, 663-671.

[13] Wu, H., Wang, H., Wang, H., Zhang, Y. and Guo, L. (2025) Numerical Simulation of Flow and Heat Transfer Characteristics in the Extrusion and Stretching Process of Non-Newtonian Fluid in Microchannel. *Chemical Engineering Science*, **306**, Article ID: 121252. https://doi.org/10.1016/j.ces.2025.121252

[14] Wajihah, S.A. and Sankar, D.S. (2023) A Review on Non-Newtonian Fluid Models for Multi-Layered Blood Rheology in Constricted Arteries. *Archive of Applied Mechanics*, **93**, 1771-1796. https://doi.org/10.1007/s00419-023-02368-6

[15] Eberhard, U., Seybold, H.J., Secchi, E., Jiménez-Martínez, J., Rühs, P.A., Ofner, A., *et al.* (2020) Mapping the Local Viscosity of Non-Newtonian Fluids Flowing through Disordered Porous Structures. *Scientific Reports*, **10**, Article No. 11733. https://doi.org/10.1038/s41598-020-68545-7

[16] Nader, E., Skinner, S., Romana, M., Fort, R., Lemonne, N., Guillot, N., *et al.* (2019)

Blood Rheology: Key Parameters, Impact on Blood Flow, Role in Sickle Cell Disease and Effects of Exercise. *Frontiers in Physiology*, **10**, Article 1329. https://doi.org/10.3389/fphys.2019.01329

[17] Wang, S., Wu, D., Li, G., Zhang, Z., Xiao, W., Li, R., *et al.* (2023) Deep Learning-Based Hemodynamic Prediction of Carotid Artery Stenosis before and after Surgical Treatments. *Frontiers in Physiology*, **13**, Article 1094743. https://doi.org/10.3389/fphys.2022.1094743

[18] Rahman, M.M., Hossain, M.A., Mamun, K. and Akhter, M.N. (2018) Comparative Study of Newtonian and Non-Newtonian Blood Flow through a Stenosed Carotid Artery. *AIP Conference Proceedings*, **1980**, Article ID: 040017. https://doi.org/10.1063/1.5044327

[19] Liu, H., Lan, L., Abrigo, J., Ip, H.L., Soo, Y., Zheng, D., *et al.* (2021) Comparison of Newtonian and Non-Newtonian Fluid Models in Blood Flow Simulation in Patients with Intracranial Arterial Stenosis. *Frontiers in Physiology*, **12**, Article 718540. https://doi.org/10.3389/fphys.2021.718540

[20] Wong, K.K.L., Wu, J., Liu, G., Huang, W. and Ghista, D.N. (2020) Coronary Arteries Hemodynamics: Effect of Arterial Geometry on Hemodynamic Parameters Causing Atherosclerosis. *Medical & Biological Engineering & Computing*, **58**, 1831-1843. https://doi.org/10.1007/s11517-020-02185-x

[21] Kumar, J.P., Sadique, M. and Shah, S.R. (2022) Mathematical Study of Blood Flow through Blood Vessels under Diseased Condition. *International Journal of Multidisciplinary Research and Development*, **9**, 31-44.

[22] Kumar, A. and Shah, S.R. (2024) Hemodynamic Simulation Approach to Understanding Blood Flow Dynamics in Stenotic Arteries. *International Journal of Scientific Research in Science and Technology*, **11**, 630-636. https://doi.org/10.32628/ijsrst241161116

[23] Akbar, S., Sharma, R.K., Sadique, M., Jaiswal, K.M., Chaturvedi, P., Kumar, V., *et al.* (2024) Computational Analysis of Clot Formation Risk in Diabetes: A Mathematical Modeling Approach. *Bibechana*, **21**, 233-240. https://doi.org/10.3126/bibechana.v21i3.64973

[24] Chaturvedi, P. and Shah, S.R. (2023) Mathematical Analysis for the Flow of Sickle Red Blood Cells in Microvessels for Bio Medical Application. *The Yale Journal of Biology and Medicine*, **96**, 13-21. https://doi.org/10.59249/atvg1290

[25] Shah, S.R. (2012) A Case Study on Non-Newtonian Viscosity of Blood through Atherosclerotic Artery. *Asian Journal of Engineering and Applied Technology*, **1**, 47-52. https://doi.org/10.51983/ajeat-2012.1.1.2501

[26] Ratan Shah, S. (2011) Non-Newtonian Flow of Blood through an Atherosclerotic Artery. *Research Journal of Applied Sciences*, **6**, 76-80. https://doi.org/10.3923/rjasci.2011.76.80

[27] Zid, I., Alilat, D., Rebhi, R., Alliche, M., Chamkha, A.J. and Zeguai, S. (2025) MHD Natural Convection of Non-Newtonian Carreau-Yasuda Nanofluid in a Square Porous Cavity by Dupuit-Darcy Model. *The European Physical Journal Plus*, **140**, Article No. 450. https://doi.org/10.1140/epjp/s13360-025-06407-9

[28] Ojha, M., Cobbold, R.S.C., Johnston, K.W. and Hummel, R.L. (1989) Pulsatile Flow through Constricted Tubes: An Experimental Investigation Using Photochromic Tracer Methods. *Journal of Fluid Mechanics*, **203**, 173-197. https://doi.org/10.1017/s0022112089001424

[29] Toufique Hasan, A.B.M. and Dipak Kanti, D. (2008) Numerical Simulation of Sinusoidal Fluctuated Pulsatile Laminar Flow through Stenotic Artery. *Journal of Applied*

Fluid Mechanics, **1**, 25-35.

[30] Lee, K.W. and Xu, X.Y. (2002) Modelling of Flow and Wall Behaviour in a Mildly Stenosed Tube. *Medical Engineering & Physics*, **24**, 575-586. https://doi.org/10.1016/s1350-4533(02)00048-6